Reprod Dom Anim **44**, 435–440 (2009); doi: 10.1111/j.1439-0531.2008.01105.x
ISSN 0936-6768

Nuclear Configuration, Spindle Morphology and Cytoskeletal Organization of *In Vivo* Maturing Horse Oocytes

MAR Siddiqui[1], EL Gastal[2], JC Ju[3], MO Gastal[1], MA Beg[2] and OJ Ginther[1,2]

[1]*Eutheria Foundation, Cross Plains, WI, USA;* [2]*Department of Pathobiological Sciences, University of Wisconsin-Madison, Madison, WI, USA;* [3]*Department of Animal Science, National Chung Hsing University, Taichung, Taiwan*

Contents

Horse oocytes (n = 37) were recovered *in vivo* from pre-ovulatory follicles 30 h after an ovulation-inducing hCG injection and were examined by fluorescent staining and confocal microscopy. Percentages of metaphase-I (MI), metaphase-II (MII) and atypical oocytes were 11%, 78% and 11% respectively. Microtubules were concentrated in the meiotic spindle in both MI and MII oocytes. Chromosomes in the metaphase plate were anchored at the equatorial region of the spindle. Spindle orientation was perpendicular to the oolema in all MI oocytes, whereas in MII oocytes, 66% were parallel and 34% were perpendicular. In MII oocytes, the nuclear material in the polar body had no specific organization and was intertwined with microtubules. Discrete foci of microfilaments at the sub-cortical region of the ooplasm formed an F-actin band, as seen in the inner confocal sections. The percentage area of oocyte image with discrete foci and/or the thickness of F-actin band was used to indicate microfilament content. Microfilament content was greater ($p < 0.006$) in MII oocytes than in MI oocytes and greater ($p < 0.03$) in MII oocytes with a perpendicular spindle than with a parallel spindle. The perpendicular spindle orientation in MII oocytes may have represented a later stage of maturation. Atypical oocytes were based on microtubules that were detached from the kinetochores and spread in the ooplasm or by microtubules that accumulated as an amorphous mass near the condensed chromatin. This is the first description of the nuclear configuration, spindle morphology and cytoskeletal organization of *in vivo* maturing horse oocytes.

Introduction

Nuclear and cytoplasmic remodelling during meiotic progression in mammals is essential for oocyte competence for fertilization and subsequent embryo development (Albertini et al. 1993). The nuclear reconfiguration during oocyte maturation is facilitated by the meiotic spindle that originated from the polymerization of tubulins to microtubules (Soifer 1986). Microfilaments are formed by the polymerization of the globular actin (G-actin) to filamentous actin (F-actin) and gives structural strength to the oocyte (Campbell et al. 1999). The oocyte competence achieved by cytoplasmic maturation involves peripheral movement of the cortical granules, rearrangement of the mitochondrial population and other organelles (Grondahl et al. 1995; Torner et al. 2007). These changes are facilitated by the microtubules and microfilaments (Sun and Schatten 2006). The final steps of oocyte maturation involve spindle rotation, anchoring of spindle to the oolema and extrusion of the polar body; all these steps are facilitated by the microfilaments (Maro et al. 1984; Terada et al. 1995; Sun and Schatten 2006).

Slaughterhouse-derived horse oocytes have been used to describe the chromatin configuration and cumulus morphology after culturing *in vitro* (Hinrichs et al. 1993, 2005; Hinrichs and Williams 1997). In other studies, oocytes that were aspirated from pre-ovulatory follicles were used for examination of the meiotic spindle morphology *in vitro* (Goudet et al. 1997), oocytes ultrastructure *in vivo* (Grondahl et al. 1995), or the initial chromatin configuration and mitochondrial aggregation after culturing *in vitro* (Torner et al. 2007). Nuclear configuration and cytoskeletal structure of *in vitro* matured horse oocytes have also been described (Tremoleda et al. 2001). To our knowledge, the combination of nuclear configuration, spindle morphology and the cytoskeletal organization of *in vivo* maturing horse oocytes have not been reported.

Oocyte maturity is often determined by the presence or absence of the first polar body in the perivitelline space (Choi et al. 2006; Ginther et al. 2007). Oocytes categorized as immature because of an absence of the first polar body most likely are at different meiotic stages before reaching MII stage. Similarly, the oocytes categorized as mature by identifying the first polar body in the perivitalline space might develop changes in spindle orientation or cytoskeleton network to reconfigure the chromatin to acquire fertilization competence. Furthermore, abnormalities in the oocyte may involve nuclear, meiotic spindle and other cytoplasmic components during maturation (Goudet et al. 1997; Delimitreva et al. 2006; Eichenlaub-Ritter et al. 2007). Stereomicroscopic examination of oocytes is limited in determining such abnormalities. Use of multiple fluorescent probes and confocal microscopy provides an effective means of simultaneous visualization of chromatin configuration, microtubules and microfilaments distribution in the oocyte (Tremoleda et al. 2001; Plancha and Albertini 1994). This experiment was performed to characterize the meiotic changes with regard to nuclear configuration, spindle morphology and cytoskeletal organization of *in vivo* maturing horse oocytes.

Materials and Methods

Source of oocytes

The oocytes (n = 37) were obtained from pony mares by transvaginal follicle aspiration during a previous study (Ginther et al. 2007). Animals were handled in accordance with the United States Department of Agriculture Guide for Care and Use of Agricultural

Animals in Agricultural Research and Teaching. Information on the mares, including feeding and experimental conditions, has been reported (Ginther et al. 2007). Briefly, mares with a growing 28 mm follicle 15 days after ovulation were scanned daily by B-mode ultrasonography until a ≥32 mm follicle was detected. Each mare with a ≥32 mm follicle was given an injection of 2500 I.U. of hCG and oocyte recovery was attempted 30 h later. Following aspiration of follicular fluid, the follicle was lavaged with 180 ml of PBS (pH 7.4, 37°C). The lavaging fluid was searched under stereomicroscope in a warm room and the oocyte was identified within 5 min after completing the recovery procedure.

Oocyte processing and staining

Unless otherwise stated, all chemicals, reagents, buffers, serum and monoclonal antibodies were purchased from Sigma-Aldrich Co. (St Louis, MO, USA). After the oocyte recovery procedure, the cumulus oocyte complex (COC) was separated from the granulosa cells and washed twice in PBS that contained 0.1% BSA. The cumulus cells were removed by treating the COC in a 25 μl drop of hyaluronidase (0.05% in PBS + 0.1% BSA) for 1 min and pipetting several times. The immunocytochemical labelling was done as described (Albertini and Clark 1981; Ju et al. 2003) with some modifications as given below. Each oocyte was processed separately to maintain the identity of the oocyte. The denuded oocyte was fixed in 150 μl of microtubule stabilizing buffer (0.5 M PIPES, 25 mM magnesium chloride, 0.01% aprotinin, 1 mM dithiothreitol, 50% deuterium oxide, 1 mM taxol, 0.1% triton-X and 2% formaline), incubated for 1 h at 38°C and stored at 4°C until immunofluorescent staining.

The fixed oocytes were washed and incubated for 2 h at 38°C in the blocking solution (2% goat serum, 2% BSA, 0.2% non-fat dry milk, 0.1 M glycine, 0.01% triton-X and 0.02% sodium azide in PBS). The oocytes were incubated with primary antibody against microtubules [dilution 1 : 200, monoclonal mouse anti-α-(Sigma catalogue # T5168) and anti-β-tubulins (Sigma catalogue # T5293)] for 4 h at 38°C. Next, the oocytes were incubated with secondary antibody conjugated with fluorescein isothiocyanate [FITC; dilution 1 : 200; goat anti-mouse antibody (catalogue # 55514), Cappel®, West Chester, PA, USA] for 1.5 h in the dark at 38°C to visualize microtubules. To visualize the microfilaments, the oocytes were incubated in phalloidin conjugated with tetramethylerhodamine isothiocyanate [TRITC; dilution 1 : 500; Rhodamin Phalloidin (catalogue # R415), Molecular Probes, Eugene, OR, USA] for 30 min in the dark at 38°C. To visualize chromatin, the oocytes were stained with Hoechst 33342 [10 μg/ml in PBS (catalogue #H1399), Molecular Probes, Eugene, OR, USA] for 15 min in the dark at 38°C. Each step of immunolabelling of the oocyte was followed by washing for 1 h in blocking solution.

Confocal microscopy and image analysis

After staining, the oocytes were mounted individually on a glass slide. To avoid excessive pressure, the cover slip was supported by droplets of paraffin–vaseline mixture placed on each of the four corners. The space between the slide and cover slip was filled with mounting media (2.5% DABCO in glycerol) and sealed with clear fingernail polish. The oocytes were examined using an inverted fluorescence microscope (Zeiss, Axiovert 200M, Carl Zeiss Microimaging Inc., Thornwood, NY, USA) that was equipped with an electron multiplying coupled charged device (EMCCD) camera and spinning Nipkow disc (Andor Technology Plc, Belfast, UK). Individual oocytes were scanned using a sequential scanning mode. Three filter sets with an excitation filter of 360 ± 20, 490 ± 10 and 555 ± 14 nm and an emission filter of 457 ± 25, 617 ± 36 and 685 ± 20 nm were engaged simultaneously to excite the Hoechst 33342, FITC and TRITC for visualization of the chromatin, microtubules and microfilaments, respectively. A complete z-stack of 20 optical sections, each section with an image resolution of 512 × 512 pixels, was acquired from individual oocytes and recorded in a computer hard disc. The microscope adjustment and the camera settings were kept constant for all oocyte evaluations.

For qualitative evaluation of the oocytes, z-stack images were analysed by ANDOR IQ imaging software (version 1.2.0, Andor Technology Plc, Belfast, UK). Meiotic spindle quality and the spindle orientation were determined by assessing the reconstructed images. For quantification of the microfilaments, z-stack images of individual oocytes were analysed by IMAGE J (version 1.32C, National Institute of Health, USA) (Rasband 2006). Briefly, an image slice from each z-stack was selected that focused the outermost surface of the oolema (plasma membrane) and depicted clear and distinct fluorescent signals emitting from the microfilaments (Fig. 1a). The 8-bit images were processed to sharpen the fluorescent signals emitted from the TRITC labelled microfilaments. A circular gate circumscribing the ooplasm of the oocyte defined the region of interest (ROI; Fig. 1b). The ROI was converted to a binary image and the percentage area of ROI with grey spots was measured to represent the content of microfilaments in the oocyte (Fig. 1c). An image slice of the equatorial section of the oocytes was selected from the z-stack images and the thickness of F-actin band of the oocyte was measured from the 12, 3, 6 and 9 o'clock positions by placing a straight line across the width of the band. The mean value of four measurements of each oocyte was used in statistical analysis.

The oocytes were grouped into metaphase-I (MI, no polar body), metaphase-II (MII, polar body) and atypical. The atypical grouping was based on microtubules that were detached from the kinetochores giving the appearance of a disorganized spindle or an accumulation of an amorphous microtubular mass near the condensed chromatin. Comparisons were made among the three groups.

Statistical analysis

The data were analysed in SAS statistical software (version 9.1.3, SAS Institute Inc., Cary, NC, USA). The microfilament content indicated by percentage area of oocyte image with discrete foci and the thickness of

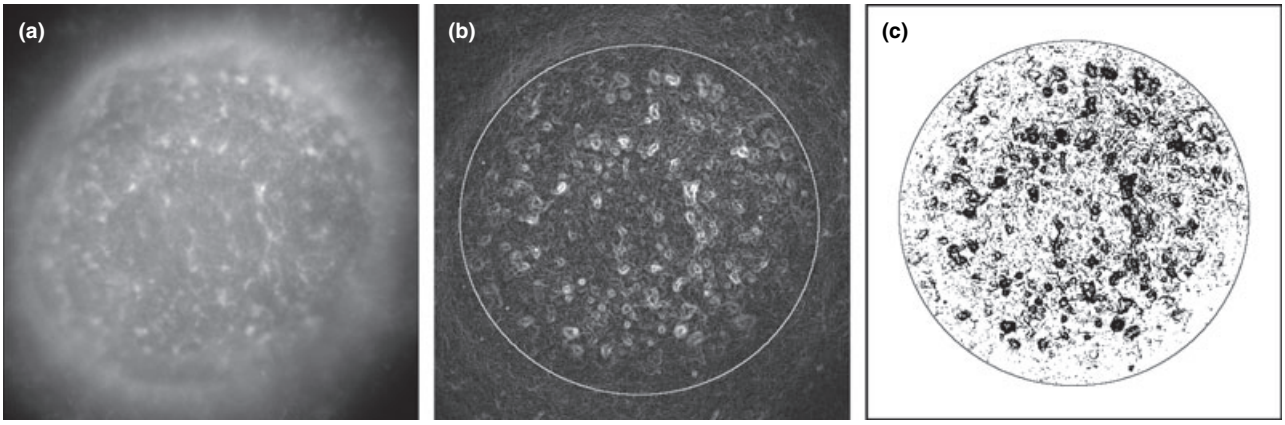

Fig. 1. Images taken during processing of an oocyte for the quantification of microfilaments. (a) Original image showing discrete foci (white spots) of the fluorescent signals emitted from the microfilaments. (b) Processed image depicting the enhanced fluorescent signals of microfilaments; the white circle circumscribing the ooplasm is the region of interest (ROI). (c) Binary image of the ROI; the percentage area in the ROI with grey spots was used to express the content of microfilaments

F-actin band of the oocyte groups (MI, MII and atypical) were analysed by general linear model (GLM) procedure for a group effect and the group means were compared with an LSD test. Frequency data for spindle orientation were analysed by chi-square test of independence. A probability of $p \leq 0.05$ indicated that a difference was significant. Frequency and discrete data are presented as percentage and mean ± SEM values, respectively.

Results

Nuclear and meiotic spindle configuration

The percentage of MI, MII and atypical oocytes was 11%, 78% and 11% respectively. The MI oocytes were characterized by the meiotic spindle and a metaphase plate (Fig. 2a). The meiotic spindle was barrel-shaped with two poles. The chromosomes were aligned on the metaphase plate and were anchored by microtubules at the equatorial region of the spindle. The spindle position of the oocyte was close to the oolema. In all MI oocytes, the meiotic spindles were positioned perpendicular to the oolema.

The MII oocytes were characterized by the presence of nuclear material on the meiotic spindle and the first polar body in the perivitelline space (Fig. 2b). The organization of the meiotic spindle and chromosomes was similar to that observed in the MI oocytes. In MII oocytes, spindle orientation was parallel and perpendicular in 66% and 34% of oocytes, respectively. The frequency of perpendicular spindle orientation in MII oocytes (Fig. 2c) was lower than in MI oocytes (Table 1). The microtubules in the polar body of the MII oocytes were intertwined with the chromatin and had no specific organization. The chromatin materials in the polar body were usually separated into clusters without any specific shape or organization (Fig. 2d).

Two of the four atypical oocytes had disorganized microtubule arrangement in the MI spindle (Fig. 2e). The disorganized microtubules appeared to be detached from the kinetochores and therefore the microtubules emanated from the spindle poles and spread into the ooplasm. The other two atypical oocytes had an accumulation of an amorphous microtubular mass near the condensed chromatin (Fig. 2f).

Microfilament distribution

Discrete foci of microfilaments that appeared as white spots at the subcortical region of the ooplasm were observed in all oocytes (Fig. 2g). Microfilaments at the subcortical region of the ooplasm were concentrated to form an F-actin band (Fig. 2h) that was observed in the inner sections of z-stack images. There was a group effect in microfilament contents (Table 1) as indicated by the area (%) of oocyte image with discrete foci ($p < 0.006$) and by F-actin band thickness of the oocyte ($p < 0.001$). Within the MII oocytes, the contents of microfilaments as percentage area with discrete foci were higher ($p < 0.03$) in oocytes with a perpendicular spindle ($n = 10$; 59.2 ± 3.3%) than in oocytes with a parallel spindle ($n = 13$; 50.9 ± 2.5%). A microfilament-rich brighter region on the actin band, the actin cap, was observed close to the meiotic spindle (Fig. 2i). The F-actin band was poorly delineated and the perivitelline space was absent in two of four atypical oocytes that had an amorphous microtubular mass near the condensed chromatin.

Discussion

There was considerable variability in the maturation stages of the oocytes at the time of recovery, but the majority (78%) had reached the MII stage. The reasons for the variability in maturation stages of oocytes may have represented, at least in part, differential response of the ≥32 mm follicles to hCG treatment (Ginther et al. 2007). The extent of *in vitro* maturation of the horse oocyte in previous studies has been inconsistent varying from 20% to 85% (Galli et al. 2007). In this study, 11% of oocytes that were arrested at the MI stage could have been cultured for a short duration for maturation progression, but the potential for the success of maturation progression of the atypical (11%) oocytes is doubtful. It is likely that the oocytes arrested at MI

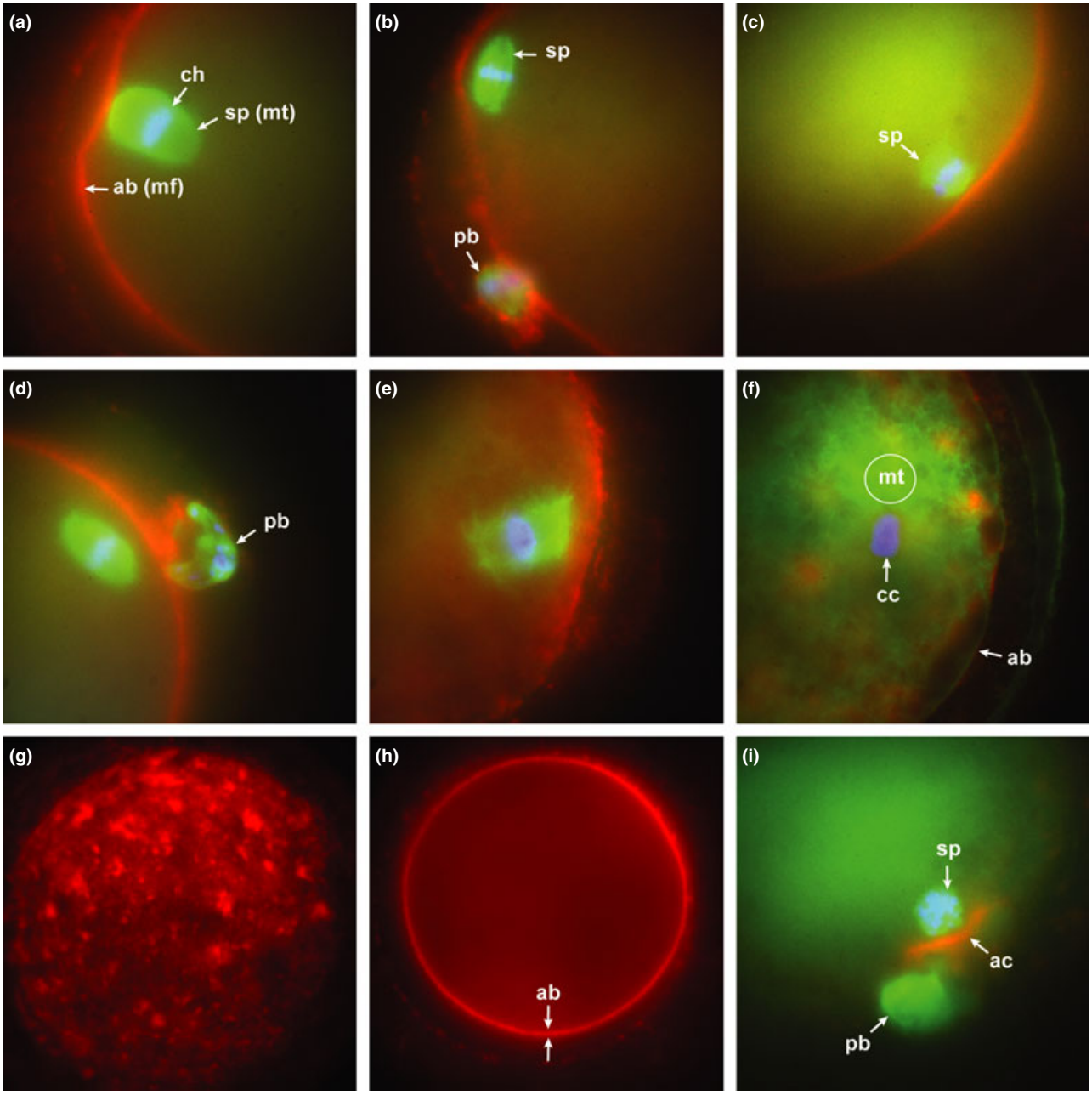

Fig. 2. Confocal microscopic images of *in vivo* maturing horse oocytes. Blue, green, and red in the color images depict the chromosomes (ch) or condensed chromatin (cc), microtubules (mt), and microfilaments (mf), respectively. Unless otherwise stated, the original magnification was ×1000. (a) An MI oocyte showing the chromosomes (ch) on the equatorial region of the meiotic spindle (sp) consisting of microtubules (mt). The spindle is oriented perpendicular to the oolema or plasma membrane at the outer margin of the actin band (ab) formed by microfilaments (mf). (b) An MII oocyte with a parallel-positioned meiotic spindle (sp) and the first polar body (pb). (c) An MII oocyte with a perpendicular positioned meiotic spindle (sp); the polar body is not seen in this plane of the image. (d) An MII oocyte with nuclear material in the polar body (pb) intertwined with the microtubules. (e) An atypical oocyte representing a disorganized MI meiotic spindle; microtubules detached from the kinetochores are emanating from the spindle poles and spread in the ooplasm. (f) Atypical oocyte representing an accumulation of an amorphous microtubular mass (mt) at the upper margin of the condensed chromatin (cc); an inconspicuous line of F-actin band (ab) and absence of perivitalline space is evident. (g) Discrete foci of microfilaments (red fluorescent signals) on the surface of an oocyte (×630). (h) An MI oocyte with F-actin band (ab, opposed arrows) surrounding the ooplasm (×630). (i) An MII oocyte with a polar body (pb) and a microfilament-rich area (actin cap; ac) close to a cross section of the meiotic spindle (sp)

stage 30 h after an hCG injection could be different than the oocytes that reached MI stage at earlier hours. However, in the present experimental design, it was not possible to ascertain this difference.

Meiotic spindles participate in nuclear remodelling and segregation of the chromosomes (Campbell et al. 1999). Thus, spindle morphology, position and orientation may be critical to the completion of meiosis. In mouse MII oocytes, the meiotic spindle is anchored parallel to the oolema by microfilaments; after sperm penetration, the spindle rotates 90° driven by the microfilaments to a position perpendicular to the oolema (Maro et al. 1984). Perpendicular orientation of the spindle is thought to facilitate the emission of the

Table 1. Characteristics of oocytes in different meiotic stages at 30 h after hCG treatment of mares

Characteristics	MI oocytes (n = 4)	MII oocytes (n = 29)	Atypical oocytes (n = 4)
Percentage of oocytes	11	78	11
Spindle orientation			
Parallel (%)	0% (0/4)[a]	65.5 (19/29)[b]	—
Perpendicular (%)	100% (4/4)[a]	34.5 (10/29)[b]	—
Microfilament contents*			
Discrete foci (% area)†	47.0 ± 1.6[a,b]	56.0 ± 2.0[a]	26.8 ± 2.0[b]
F-actin band thickness (μm)	0.48 ± 0.06[a]	0.55 ± 0.01[b]	0.39 ± 0.09[c]

MI, metaphase I; MII, metaphase II. Within a row, values with different superscripts differ ($p < 0.02$).
†Only 23 oocyte images of MII oocytes were available for the microfilament evaluation.
*Percentage of the oocyte area with fluorescent signals emitted from microfilaments as indicated by grey spots after processing of oocyte image.

polar body from the action of microfilaments. In other mammals, the spindle is oriented perpendicularly in the MII oocytes (Sun and Schatten 2006). However, all of the MI oocytes but only 10 of 29 MII oocytes in this *in vivo* study had perpendicular spindles. The role of spindle orientation in horse oocytes has not been studied by either *in vitro* or *in vivo* systems.

In this study, the microfilament content of the oocytes was considered as an indicator of the cytoplasmic maturation of the oocytes. Rotation of spindle at the final stage of meiotic changes and sperm incorporation at fertilization are facilitated by the microfilaments (Maro et al. 1984; Le Guen et al. 1989; Sun and Schatten 2006). The greater thickness of the F-actin band in MII vs MI oocytes, in this study, represents greater microfilament content in the MII oocytes, indicating that the microfilaments are involved in cytoplasmic maturation. Greater microfilament content in the MII oocytes with perpendicular spindles than in the oocytes with parallel spindles suggests that the perpendicular spindles represent a later stage of oocyte maturity. That is, the parallel spindles had not yet rotated to the perpendicular form that precedes extrusion of the second polar body. Although not previously reported for equine oocytes, these considerations have been noted for other species (Maro et al. 1986; Gard et al. 1995; Zhong et al. 2005).

Two of the four atypical oocytes represented detachment of microtubules from the kinetochores in the spindle. Goudet et al. (1997) reported similar disarrangement in the meiotic spindle of equine oocytes and proposed that such disarrangement could be a normal transitional step in microtubule dynamics during meiotic progression. However, similar abnormal spindle arrangements were also reported in aged or heat exposed human (Almeida and Bolton 1995), mouse (Sun et al. 2004), pig (Liu et al. 2003) and cattle (Ju et al. 2005) oocytes that were matured *in vitro*. The abnormalities/disorganizations of the microtubules in the meiotic spindle of the oocytes in this study may have had an abnormal or detrimental microtubule organization. The two other atypical oocytes represented an accumulation of an amorphous microtubular mass at the margin of the condensed chromatin. A compact nucleus, absence of perivitaline space and presence of a very thin line of F-actin band in these oocytes suggest that they might have been at GV stage (Tremoleda et al. 2001). However, such accumulation of microtubule was not reported in slaughterhouse-derived horse oocytes until the germinal vesicle breakdown stage after 12 h of culture (Tremoleda et al. 2001). Microtubule aggregation at the GV stage has been reported in human (Kim et al. 1998), rabbit (Ju et al. 2002) and mouse oocytes (Mattson and Albertini 1990) but in the pig oocytes such accumulation of microtubules was not detected (Brevini et al. 2007). Microtubules are highly temperature sensitive and depolymerization may occur because of temperature fluctuation during oocyte handling. Although, in this study, precaution was taken to minimize temperature variations, inadvertent fluctuations could have occurred. However, it was not possible to determine if these findings resulted from temperature related to depolymerization of spindle forming microtubules or represented a microtubule organizing centre. It is notable that the increasing follicle diameter, color Doppler signals of blood flow, B-mode ultrasonographic morphology and lower percentage of apoptotic granulosa cells in these follicles, as reported previously (Ginther et al. 2007), indicated that the oocytes of this study were not derived from degenerated follicles.

In this study, 11% of the recovered oocytes that were grouped as atypical had apparent abnormalities. Normality of the recovered oocytes (89%; MI and MII) of this study is similar to a reported 91% fertilization rate of ovulated oocytes that were obtained from the oviducts (Peyrot et al. 1987). Thus, 11% of oocytes classified as atypical may correspond to the reported rate of unfertilization. It has been suggested that fertilization and subsequent embryo development are adversely affected because of spindle abnormalities in the oocyte (Ju et al. 2005). In conclusion, this study provided a basis for the understanding of the nuclear and cytoskeletal organization of *in vivo* maturing horse oocytes and demonstrated the distribution of the microtubules and microfilaments in normal and in apparently abnormal oocytes.

Acknowledgements

The project was supported by Eutheria Foundation, Cross Plains, WI (Project P2-OG-06). The authors thank Dr Ralph M. Albrecht, Director of Biological & Biomaterials Preparation, Imaging and Characterization (BBPIC) facility at the University of Wisconsin-Madison for the use of confocal microscope and Joseph Heintz for assistance during imaging.

References

Albertini DF, Clark JI, 1981: Visualization of assembled and disassembled microtubule protein by double label fluorescence microscopy. Cell Biol Int Rep **5,** 387–397.

Albertini DF, Wickramasinghe D, Messinger S, Mattson BA, Plancha CE, 1993: Nuclear and cytoplasmic changes during oocyte maturation. In: Bavister BD (ed.), Preimplantation Embryo Development. Springer-Verlag, New York, pp. 3–21.

Almeida PA, Bolton VN, 1995: The effect of temperature fluctuations on the cytoskeletal organization and chromosomal constitution of the human oocyte. Zygote **3,** 357–365.

Brevini TA, Cillo F, Antonini S, Gandolfi F, 2007: Cytoplasmic remodeling and the acquisition of developmental competence in pig oocytes. Anim Reprod Sci **98,** 23–38.

Campbell NA, Reece JB, Mitchell GL, 1999: A tour of the cell. In: Mulligan E (ed.), Biology. 5th edn. Addison Wesley Longman Inc., California, pp. 102–129.

Choi YH, Love LB, Varner DD, Hinrichs K, 2006: Holding immature equine oocytes in the absence of meiotic inhibitors: effect on germinal vesicle chromatin and blastocyst development after intracytoplasmic sperm injection. Theriogenology **66,** 955–963.

Delimitreva S, Zhivkova R, Isachenko E, Umland N, Nayudu PL, 2006: Meiotic abnormalities in *in vitro*-matured marmoset monkey (*Callithrix jacchus*) oocytes: development of a non-human primate model to investigate causal factors. Hum Reprod **21,** 240–247.

Eichenlaub-Ritter U, Winterscheidt U, Vogt E, Shen Y, Tinneberg HR, Sorensen R, 2007: 2-methoxyestradiol induces spindle aberrations, chromosome congression failure, and nondisjunction in mouse oocytes. Biol Reprod **76,** 784–793.

Galli C, Colleoni S, Duchi R, Lagutina I, Lazzari G, 2007: Developmental competence of equine oocytes and embryos obtained by *in vitro* procedures ranging from *in vitro* maturation and ICSI to embryo culture, cryopreservation and somatic cell nuclear transfer. Anim Reprod Sci **98,** 39–55.

Gard DL, Cha BJ, Roeder AD, 1995: F-actin is required for spindle anchoring and rotation in *Xenopus* oocytes: a re-examination of the effects of cytochalasin B on oocyte maturation. Zygote **3,** 17–26.

Ginther OJ, Gastal EL, Gastal MO, Siddiqui MAR, Beg MA, 2007: Relationship of follicle vs oocyte maturity to ultrasound morphology, blood flow and hormone concentrations of the preovulatory follicle in mares. Biol Reprod **77,** 202–208.

Goudet G, Bezard J, Duchamp G, Gerard N, Palmer E, 1997: Equine oocyte competence for nuclear and cytoplasmic *in vitro* maturation: effect of follicle size and hormonal environment. Biol Reprod **57,** 232–245.

Grondahl C, Hyttel P, Grondahl ML, Eriksen T, Gotfredsen P, Greve T, 1995: Structural and endocrine aspects of equine oocyte maturation *in vivo*. Mol Reprod Dev **42,** 94–105.

Hinrichs K, Williams KA, 1997: Relationships among oocyte-cumulus morphology, follicular atresia, initial chromatin configuration, and oocyte meiotic competence in the horse. Biol Reprod **57,** 377–384.

Hinrichs K, Schmidt AL, Friedman PP, Selgrath JP, Martin MG, 1993: *In vitro* maturation of horse oocytes: characterization of chromatin configuration using fluorescence microscopy. Biol Reprod **48,** 363–370.

Hinrichs K, Choi YH, Love LB, Varner DD, Love CC, Walckenaer BE, 2005: Chromatin configuration within the germinal vesicle of horse oocytes: changes post mortem and relationship to meiotic and developmental competence. Biol Reprod **72,** 1142–1150.

Ju JC, Chen TH, Tseng JK, Tsay C, Yeh SP, Chou PC, Chen CH, Liu CT, 2002: Cytoskeletal patterns, *in vitro* maturation and parthenogenetic development of rabbit GV oocytes. Asian-Aust J Anim Sci **15,** 1695–1701.

Ju JC, Tsay C, Ruan CW, 2003: Alterations and reversibility in the chromatin, cytoskeleton and development of pig oocytes treated with roscovitine. Mol Reprod Dev **64,** 482–491.

Ju JC, Jiang S, Tseng JK, Parks JE, Yang X, 2005: Heat shock reduces developmental competence and alters spindle configuration of bovine oocytes. Theriogenology **64,** 1677–1689.

Kim NH, Chung HM, Cha KY, Chung KS, 1998: Microtubule and microfilament organization in maturing human oocytes. Hum Reprod **13,** 2217–2222.

Le Guen P, Crozet N, Huneau D, Gall L, 1989: Distribution and role of microfilaments during early events of sheep fertilization. Gamete Res **22,** 411–425.

Liu RH, Sun QY, Li YH, Jiao LH, Wang WH, 2003: Effects of cooling on meiotic spindle structure and chromosome alignment within *in vitro* matured porcine oocytes. Mol Reprod Dev **65,** 212–218.

Maro B, Johnson MH, Pickering SJ, Flach G, 1984: Changes in actin distribution during fertilization of the mouse egg. J Embryol Exp Morphol **92,** 11–32.

Maro B, Johnson MH, Pickering SJ, Flach G, 1986: Mechanism of polar body formation in the mouse oocyte: an interaction between the chromosomes, the cytoskeleton and plasma membrane. J Embryol Exp Morphol **92,** 11–32.

Mattson BA, Albertini DF, 1990: Oogenesis: Chromatin and microtubule dynamics during the meiotic prophase. Mol Reprod Dev **25,** 374–383.

Peyrot LM, Little TV, Lowe JE, Weber JA, Woods GL, 1987: Autotransfer of day 4 embryos from oviduct to oviduct vs oviduct to uterus in mares. Theriogenology **28,** 699–708.

Plancha EC, Albertini DF, 1994: Hormonal regulation of meiotic maturation in the hamster oocyte involves a cytoskeleton-mediated process. Biol Reprod **51,** 852–864.

Rasband WS, 2006: Image J. US National Institute of Health, Bethesda, MD, USA. Available: http://rsb.info.nih.gov/ij/ (accessed 10 June 2007).

Soifer D, 1986: Factors regulating the presence of microtubules in cells. Ann N Y Acad Sci **466,** 1–7.

Sun QY, Schatten H, 2006: Regulation of dynamic events by microfilaments during oocyte maturation and fertilization. Reproduction **131,** 193–205.

Sun XF, Zhang WH, Chen XJ, Xiao GH, Mai WY, Wang WH, 2004: Spindle dynamics in living mouse oocytes during meiotic maturation, ageing, cooling and overheating: a study by polarized light microscopy. Zygote **12,** 241–249.

Terada Y, Fukaya T, Yajima A, 1995: Localization of microfilaments during oocyte maturation of golden hamster. Mol Reprod Dev **42,** 486–492.

Torner H, Alm H, Kanitz W, Goellnitz K, Becker F, Poehland R, Bruessow KP, Tuchscherer A, 2007: Effect of initial cumulus morphology on meiotic dynamic and status of mitochondria in horse oocytes during IVM. Reprod Domest Anim **42,** 176–183.

Tremoleda JL, Schoevers EJ, Stout TAE, Colenbrander B, Bevers MM, 2001: Organization of the cytoskeleton during *in vitro* maturation of horse oocytes. Mol Reprod Dev **60,** 260–269.

Zhong ZS, Huo LJ, Liang CG, Chen DY, Sun QY, 2005: Small GTPase RhoA is required for ooplasmic segregation and spindle rotation, but not for spindle organization and chromosome separation during mouse oocyte maturation, fertilization, and early cleavage. Mol Reprod Dev **71,** 256–261.

Submitted: 15 Feb 2008

Author's address (for correspondence): OJ Ginther, Department of Pathobiological Sciences, University of Wisconsin-Madison, 1656 Linden Drive, Madison, WI 53706, USA. E-mail: ginther@svm.vetmed.wisc.edu